Proceedings of HT2005
2005 ASME Summer Heat Transfer Conference
July 17-22, 2005, San Francisco, California, USA

HT2005-72581

HEAT TRANSFER DYNAMICS DURING TREATMENT OF PORT WINE STAIN BIRTHMARKS WITH MULTIPLE-INTERMITTENT CRYOGEN SPURTS AND LASER PULSES

Wangcun Jia[1], Guillermo Aguilar[1,2], and J. Stuart Nelson[1]
[1]Beckman Laser Institute, University of California, Irvine, CA 92612
[2]Department of Mechanical Engineering, University of California, Riverside, CA 92521

ABSTRACT

Port wine stain (PWS) is a congenital, progressive vascular malformation of human skin. Presently, all PWS patients are treated using single cryogen spurt and single laser pulse exposure (SCS-SLP), which does not produce complete lesion blanching in the vast majority of patients. In this study, the feasibility of applying multiple cryogen spurts intermittently with multiple laser pulse exposures (MCS-MLP) is studied numerically. Laser therapy of PWS was simulated with finite element heat diffusion and Monte Carlo light distribution models. Epidermal and thermal damage of PWS blood vessels of various diameters (50 – 130 μm) were calculated with an Arrhenius-type kinetic model. The results show that the proposed MCS-MLP approach can provide sufficient epidermal protection while at the same time achieving higher core intravascular temperatures over longer periods of time. PWS patients may benefit from the MCS-MLP approach, depending on PWS vessels diameter.

INTRODUCTION

Port wine stain (PWS) is a congenital, progressive vascular malformation of human skin. The pulsed dye laser produces reasonably good results in a select population of PWS patients due to its ability to destroy cutaneous blood vessels selectively. However, non-specific absorption by epidermal melanin competes for absorption of laser radiation in subsurface target chromophores. If not controlled, high epidermal temperatures can lead to blistering, dyspigmentation or scarring and thus limit the laser radiant exposure that can be safely applied. An important approach to the aforementioned problem is to cool the most superficial layers of the skin selectively with cryogen spurt, which has led to improved therapeutic outcome of PWS and other vascular lesions [1-8]. However, the current approach with single cryogen spurt and single laser pulse exposure (SCS-SLP) does not produce complete lesion blanching in the vast majority of patients [9]. The principal reason is that heat generation within large PWS vessels is constrained to the upper portion thereof because the light penetration depth is too short in blood at the wavelengths (585-595 nm) currently used for therapy. Multiple cryogen spurts applied intermittently with multiple laser pulse exposures (MCS-MLP) has the potential to gradually heat up the targeted PWS vessels while at the same time maintaining the epidermal temperature below its threshold for damage.

Previous studies [10, 11] have proven the utility of applying intermittent cryogen spurts along with continuous laser irradiation to cause deeper tissue photocoagulation using a Nd:YAG laser (λ=1064 nm). A subsequent study by Verkruysse et al [12] introduced a mathematical model that supports the use of multiple laser pulses as a means to target optically shielded blood vessels, which fail to respond to the current approach of a single laser pulse. Using a finite difference heat diffusion and multilayer Monte Carlo light distribution numerical model, Aguilar et al [13] investigated the possibility of using the MCS-MLP to overcome the excessive epidermal heating during high fluence therapeutic procedures of SCS-SLP approach. In that model, the skin was simulated as four layers and vessels were simulated as a homogeneous distribution of blood. In the present study, a more realistic multiple cylindrical blood vessels model of PWS skin is used to investigate the effect of MCS-MLP as a function of skin type and size of the blood vessels. Moreover, experimentally determined dynamic heat flux (q'') induced by a cryogen spurt [14] was used as the thermal boundary condition required in the simulation of cryogen spurt–assisted laser therapy of PWS.

NUMERICAL MODELS

The numerical models illustrated in Figure 1 have three main components: a Monte Carlo (MC) light distribution model, a finite-element solution to the heat-conduction equation, and an Arrhenius rate process integral to calculate thermal damage. The MC model simulates light transport in human skin to produce energy deposition per unit time per unit skin volume during laser pulse exposure, $S(r, z, t)$, where r and z are lateral and depth dimensions, respectively. The thermal diffusion model simulates heat transfer in human skin during cooling, pulsed laser exposure and thermal relaxation phase to compute the time-dependent temperature distribution within human skin. The Arrhenius rate process model simulates tissue denaturation to predict epidermal thermal damage and blood

photocoagulation. Each of these models is described in detail below.

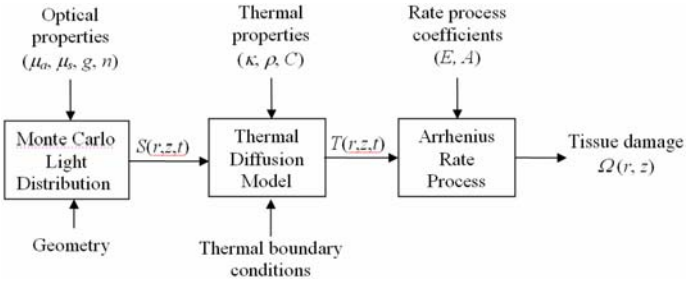

Figure 1: Block diagram of the numerical models.

The MC model used in this study was developed by Keijzer et al. [15-17] and the details will not be repeated here. The skin is modeled by two infinitely wide layers representing the epidermis and dermis of 50 μm and 950~1450 μm thicknesses, respectively (see Figure 2). Vessels with six different diameters, ranging from 50-130 μm are placed in the dermis 300~500 μm below the skin surface. The distribution of the vessels shown in Figure 2 is extended infinitely to the left and right. We simulate an incident laser beam of infinite diameter, which is a good approximation for the spot size in current clinical use [16, 18]. The wavelength in our simulation is 532 nm rather than 585 or 595 nm because the prototype laser capable of operating at the high repetition rate required to increase the vessels temperature with successive laser pulses is a frequency-doubled Nd:YAG laser. The optical properties at 532 nm for each skin component [19] are listed in Table 1. In our model, melanin is homogeneously distributed in the epidermis and the volume fraction is 5 and 10%, which approximately correspond to lightly and moderately pigmented patients, respectively. Blood is represented by the optical properties of hemoglobin (Hb). We assume the hematocrit is 40% and the hemoglobin is distributed homogeneously in the vessel.

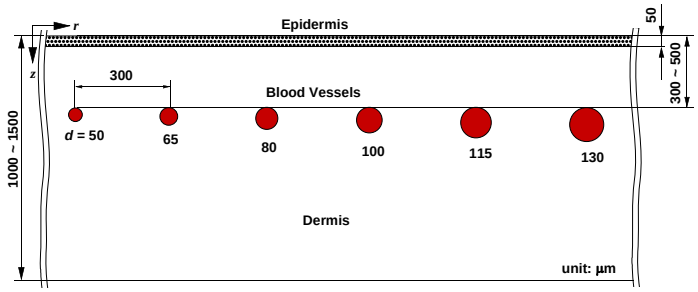

Figure 2: Geometries of human skin model with discrete PWS blood vessels.

Table 1: Optical properties of various skin components used in the Monte Carlo model

Skin component	μ_a (1/cm)	μ_s (1/cm)	g
Epidermis	27, 54	530	0.77
Dermis	2.7	156	0.77
Blood	266	473	0.99

The two-dimensional transient heat-conduction equation

$$\kappa\nabla^2 T(r,z,t) + S(r,z) = \rho c \frac{\partial T(r,z,t)}{\partial t} \qquad (2)$$

is solved with a finite element method (FEM) using a commercial package, FEMLAB®. Heat transfer owing to blood perfusion was neglected because that effect is not important on the short time scales (i.e., hundreds of milliseconds) used in this study [20]. The thermal properties of skin [14, 21] used in this model are listed in Table 2. The heat-source term, S, is present only during pulsed laser exposure, t_p. A constant initial temperature of 35°C is used for the entire tissue volume. Adiabatic boundary conditions are applied at $z = \infty$ and $r = \pm\infty$. At the surface of the skin model, the thermal boundary condition changes with time. During the effective cooling period of cryogen spurt (spurt duration plus cryogen residual time), the experimentally determined heat flux is used [14]. After exposure of the last laser pulse, a natural convection heat transfer coefficient of 10 W/(m^2·°C) and an ambient temperature of 25°C are used.

Table 2: Thermal properties of various skin components used in the heat transfer model

Skin component	κ (W/m·K)	ρ (kg/m^3)	c (J/kg·K)
Epidermis	0.34	1120	3200
Dermis	0.41	1090	3500
Blood	0.55	1060	3600

To account for the latent heat of vaporization of tissue water during laser irridiation, c in Eq.2 is replaced by (c + $D\Delta H$). ΔH is the latent heat of vaporization, and D is defined as a normalized Gaussian pulse (having unity integral), according to the following equation:

$$D = \frac{\exp\left(\frac{-(T-T_B)^2}{\nabla T^2}\right)}{\sqrt{\pi\nabla T^2}} \qquad (3)$$

where T_B is the temperature at which the rate of water vaporization maximizes and ΔT is the half width of the temperature interval between the start, and the end, of vaporization. In our simulation, T_B is 108°C to account for the blood superheat before vaporization and ΔT = 2.5°C is selected arbitrarily.

The Arrhenius rate process integral is used to quantify tissue thermal damages:

$$\Omega(r,z,\tau) = \ln\left[\frac{C_n(r,z,0)}{C_n(r,z,\tau)}\right] = A\int_0^\tau \left\{\exp\left[-\frac{\Delta E}{RT(r,z,t)}\right]dt\right\} \qquad (4)$$

where C_n is the remaining concentration of native tissue at exposure time t, τ is the total procedure time, and R is the universal gas constant (8.314 J/(mole·K)). We use the values A = 1.8 x 10^{51} s^{-1} and ΔE = 327,000 J/mole for bulk skin [22] and A = 7.6 x 10^{66} s^{-1} and ΔE = 455,000 J/mole for blood [23]. Calculations of Ω are maintained for a period of time after laser irradiation until thermal damage accumulation has ceased.

RESULTS AND DISCUSSIONS

Simulated Temperature Distribution

For the SCS-SLP simulation, we assume a SCS of 100 ms followed by a SLP of 1 ms. For MCS-MLP, we also assume an initial cryogen spurt of 100 ms followed by a sequence of six 1 ms MLP and five 49 ms MCS applied intermittently, which effectively provide a *repetition rate* of 20 Hz. The assumed

melanin volume fraction (MVF) in the epidermis is 10% (which represents a moderately pigmented skin type patient), blood vessels are located 300 μm below the surface and laser fluence is 3.5 J/cm^2 for both SLP and MLP.

Since the epidermal-dermal junction (basal layer) is the region that requires the most effective thermal protection, we show in Figure 3a the temperature variation with time at z = 50 μm. As a representative of the intravascular core temperature we show in Figure 3b the temperature variation with time at the center of an 130 μm diameter vessel (z = 300 μm). Note that the epidermal-dermal junction remains below 70°C because MCS remove epidermal heat fast enough avoiding excessive epidermal damage [14]. Meanwhile, the vessel center temperature is consistently increased with each consecutive laser pulse. Figure 4 shows the temperature profiles across the center of an 80 μm diameter blood vessel as a function of depth at the end of the first and sixth laser pulse. It is shown clearly that the temperature in the epidermis is maintained below a threshold temperature of 70°C while the temperatures in the top portion of the blood vessel are maintained at T_B for both. However, blood vessels are heated more uniformly with MLP.

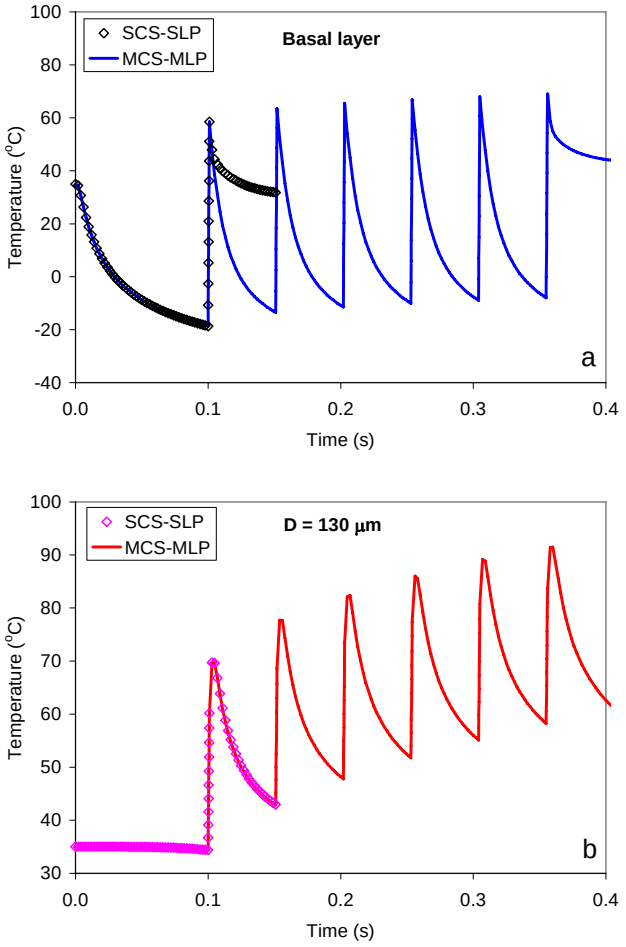

Figure 3: Temperature variation with time at the basal layer (a) and center of 130 μm diameter vessel (b) MVF = 10%; PWS depth, 300 μm; laser repetition rate, 20 Hz, 3.5 J/cm^2, 1.5 ms.

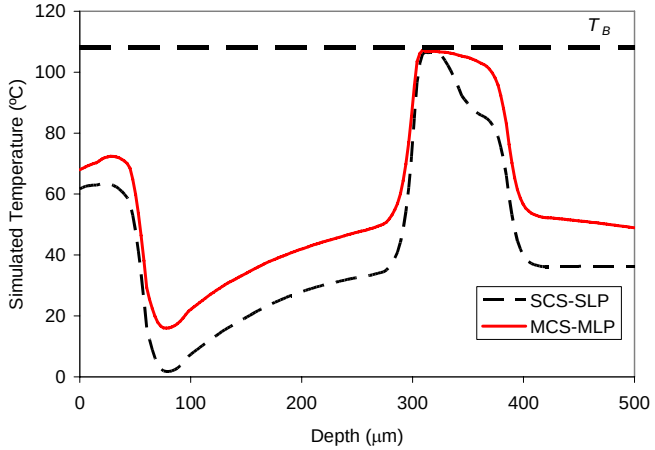

Figure 4: Temperature profiles as a function of depth at the end of the first and the sixth laser pulse, MVF = 10%; PWS depth, 300 μm; laser repetition rate, 20 Hz, 3.5 J/cm^2, 1.5 ms.

Simulated Photo-Coagulation

A color map of calculated Ω values for model skin using the Arrhenius rate process integral with SCS-SLP is shown in Figure 5. The MVF, PWS vessel depth, cooling and laser parameters are the same as above. The scale of Ω is set from zero to four to make the color map easy to read because Ω = 4 already corresponds to a 98% decrease from the original total of undamaged tissue constituents. The damage threshold for tissue necrosis is selected as Ω =1 (a 63% decrease from the original total of undamaged tissue constituents). It can be seen there is no sign of epidermal injury at a laser fluence of 3.5 J/cm^2. However, if laser fluence is increased to 4.0 J/cm^2, epidermal injury is predicted by our simulation (not shown). As for blood vessel damage, we need to define a criterion to assess irreversible vessel damage. Previous theoretical models used threshold average temperature of 70°C to predict vessel necrosis [24]. However, in vitro laser irradiation of whole blood showed that blood coagulation occurs at 80-90°C [25]. Instead of a threshold average temperature, the area ratio of coagulated blood to total blood in the vessel (r_c) is selected to assess irreversible vessel damage. If this ratio is higher than 64%, we assume the vessel is destroyed irreversibly [26].

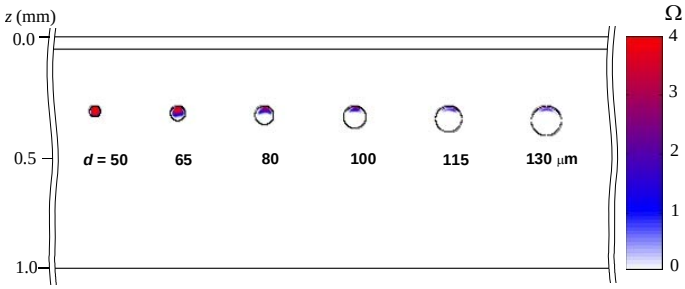

Figure 5: Color map of calculated Ω values for the model skin with SCS-SLP, MVF = 10%; PWS depth, 300 μm.

Figure 6 shows r_c for vessels of different diameters with SCS-SLP and MCS-MLP. The laser fluence was 3.5 J/cm^2 for both simulations and no epidermal injury is predicted. It can be

seen that r_c for large vessels (> 80 μm diameter) increase substantially from an average of 6% for SCS-SLP to 57% for MCS-MLP. Based on the damage criterion we assumed, vessels of diameter less than 50 μm are destroyed irreversibly with SCS-SLP. However, treatable vessel diameter increases to 80 μm with MCS-MLP.

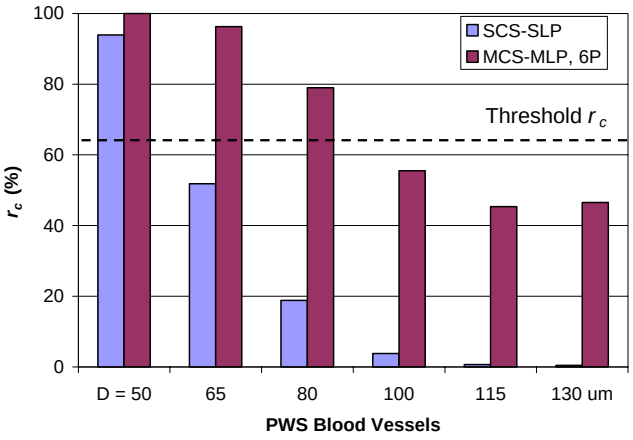

Figure 6: r_c for vessels of different diameters with SCS-SLP and MCS-MLP, MVF = 10%; PWS depth, 300 μm.

Figure 7 shows r_c for vessels of different diameters with SCS-SLP and MCS-MLP when the MVF is 5%, which represents a light skin type patient. Depth of PWS vessels is 500 μm. The laser fluence was 5 J/cm^2 (the maximum allowed to avoid epidermal injuries for both simulations). It can be seen that r_c for large vessels (> 80 μm diameter) increase nearly 2 times from an average of 47% for SCS-SLP to 88% for MCS-MLP. Based on the damage criterion we assumed, vessels of diameter less than 80 μm are destroyed irreversibly with SCS-SLP. However, treatable vessel diameter increases to 130 μm with MCS-MLP.

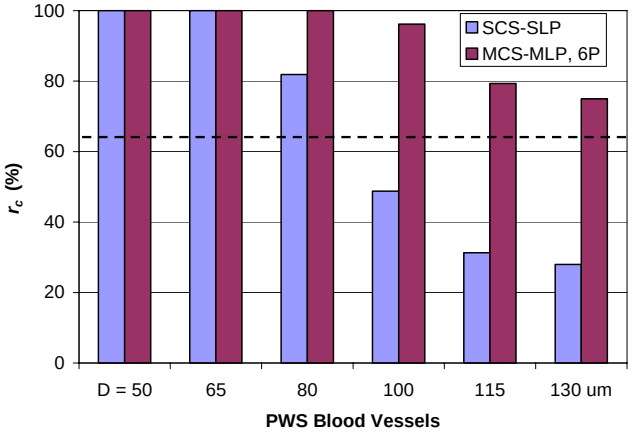

Figure 7: r_c for vessels of different diameters with SCS-SLP and MCS-MLP, MVF = 5%; PWS depth, 500 μm.

Discussions

Our numerical results show that the temperature in the top portion of the blood vessel is maintained at T_B for both SLP and MLP. The reason is that significant vaporization of water in blood is assumed to occur at T_B. Blood temperature will exceed T_B only after all water is vaporized. Although the actual T_B is not known, it is likely that it is higher than what we assumed because the very high heating rate and pressure increase in confined vessels. One piece of experimental evidence is that blood temperature reached 150°C before significant explosive vaporization occurred during open-cuvette pulsed laser irradiation of whole blood [25]. In fact, higher T_B would favor the MCS-MLP approach because the gap between T_B and the maximum blood temperature with SLP would be enlarged and higher blood temperature could be achieved with MLP before it reaches T_B.

The effect of MCS-MLP on laser therapeutic outcome depends greatly on PWS blood vessel morphology. Qualitatively, MCS-MLP will improve the therapeutic outcome of a PWS lesion with large ectatic vessels. Quantitative prediction of the therapeutic outcome with MCS-MLP can only be reached when the criterion to assess irreversible PWS vessel damage is well defined. Therefore, further experimental validation and clinical studies of the MCS-MLP are urgently needed to assess the role of such an approach to the clinical management of patients with PWS.

CONCLUSIONS

Using heat diffusion, light distribution, and thermal damage computational models, it is shown that multiple-intermittent cryogen spurts and laser pulses (MCS-MLP approach) could provide sufficient epidermal protection while, at the same time, achieve higher core intravascular temperatures over longer periods of time. PWS patients may benefit from the MCS-MLP approach, depending on PWS vessels diameter. The validity of the MCS-MLP approach should be eventually confirmed through clinical trials and histological characterization.

ACKNOWLEDGMENTS

The authors would like to thank Dr. Jenny Zhang for discussions regarding the numerical models. This work was supported by the National Institutes of Health (GM 62177 and AR 47551 to JSN and HD42057 to GA) and UCR Academic Senate Grant to GA. Institutional support from the Beckman Laser Institute Endowment is also acknowledged.

REFERENCES

1. Nelson, JS, Milner, TE, Anvari, B, Tanenbaum, BS, Kimel, S, Svaasand, LO, and Jacques, SL, *Dynamic Epidermal Cooling During Pulsed-Laser Treatment of Port-Wine Stain - a New Methodology with Preliminary Clinical-Evaluation.* Archives of Dermatology, 1995. **131**(6): p. 695-700.

2. Nelson, JS, Milner, TE, Anvari, B, Tanenbaum, S, Svaasand, LO, and Kimel, S, *Dynamic epidermal cooling in conjunction with laser-induced photothermolysis of port wine stain blood vessels.* Lasers in Surgery and Medicine, 1996. **19**(2): p. 224-229.

3. Waldorf, HA, Alster, TS, McMillan, K, Kauvar, ANB, Geronemus, RG, and Nelson, JS, *Effect of dynamic cooling on 585-nm pulsed dye laser treatment of port-*

wine stain birthmarks. Dermatologic Surgery, 1997. **23**(8): p. 657-662.

4. Chang, CJ and Nelson, JS, *Cryogen spray cooling and higher fluence pulsed dye laser treatment improve port-wine stain clearance while minimizing epidermal damage.* Dermatologic Surgery, 1999. **25**(10): p. 767-772.
5. Chang, CJ, Anvari, B, and Nelson, JS, *Cryogen spray cooling for spatially selective photocoagulation of hemangiomas: A new methodology with preliminary clinical reports.* Plastic and Reconstructive Surgery, 1998. **102**(2): p. 459-463.
6. Chang, CJ, Kelly, KM, and Nelson, JS, *Cryogen spray cooling and pulsed dye laser treatment of cutaneous hemangiomas.* Annals of Plastic Surgery, 2001. **46**(6): p. 577-583.
7. Fiskerstrand, EJ, Ryggen, K, Norvang, LT, and Svaasand, LO, *Clinical effects of dynamic cooling during pulsed laser treatment of port-wine stains.* Lasers in Medical Science, 1997. **12**(4): p. 320-327.
8. Chiu, CH, Chan, HHL, Ho, WS, Yeung, CK, and Nelson, JS, *Prospective study of pulsed dye laser in conjunction with cryogen spray cooling for treatment of port wine stains in Chinese patients.* Dermatologic Surgery, 2003. **29**(9): p. 909-915.
9. van der Horst, CMAM, Koster, PHL, de Borgie, CAJM, Bossuyt, PMM, and van Gemert, MJC, *Effect of the timing of treatment of port-wine stains with the flash-lamp-pumped pulsed dye-laser.* New England Journal of Medicine, 1998. **338**(15): p. 1028-1033.
10. Anvari, B, Tanenbaum, BS, Milner, TE, Tang, K, Liaw, LH, Kalafus, K, Kimel, S, and Nelson, JS, *Spatially selective photocoagulation of biological tissues: Feasibility study utilizing cryogen spray cooling.* Applied Optics, 1996. **35**(19): p. 3314-3320.
11. Anvari, B, Tanenbaum, BS, Hoffman, W, Said, S, Milner, TE, Liaw, LH, and Nelson, JS, *Nd:YAG laser irradiation in conjunction with cryogen spray cooling induces deep and spatially selective photocoagulation in animal models.* Phys Med Biol, 1997. **42**(2): p. 265-82.
12. Verkruysse, W, van Gemert, MJC, Smithies, DJ, and Nelson, JS, *Modelling multiple laser pulses for port wine stain treatment.* Physics in Medicine and Biology, 2000. **45**(12): p. N197-N203.
13. Aguilar, G, Diaz, SH, Lavernia, EJ, and Nelson, JS, *Cryogen spray cooling efficiency: Improvement of port wine stain laser therapy through multiple-intermittent cryogen spurts and laser pulses.* Lasers in Surgery and Medicine, 2002. **31**(1): p. 27-35.
14. Jia, W, Aguilar, G, Verkruysse, W, Franco, W, and Nelson, JS, *Improvement of Port Wine Stain Laser Therapy by Skin Preheating prior to Cryogen Spray Cooling: a Numerical Simulation.* submitted to Lasers in Surgery and Medicine, 2004.
15. Keijzer, M, Jacques, SL, Prahl, SA, and Welch, AJ, *Light Distributions in Artery Tissue - Monte-Carlo Simulations for Finite-Diameter Laser-Beams.* Lasers in Surgery and Medicine, 1989. **9**(2): p. 148-154.
16. Keijzer, M, Pickering, JW, and van Gemert, MJC, *Laser-Beam Diameter for Port Wine Stain Treatment.* Lasers in Surgery and Medicine, 1991. **11**(6): p. 601-605.
17. Lucassen, GW, Verkruysse, W, Keijzer, M, and van Gemert, MJC, *Light distributions in a port wine stain model containing multiple cylindrical and curved blood vessels.* Lasers in Surgery and Medicine, 1996. **18**(4): p. 345-357.
18. Verkruysse, W, Lucassen, GW, deBoer, JF, Smithies, DJ, Nelson, JS, and van Gemert, MJC, *Modelling light distributions of homogeneous versus discrete absorbers in light irradiated turbid media.* Physics in Medicine and Biology, 1997. **42**(1): p. 51-65.
19. Verkruysse, W, Pickering, JW, Beek, JF, Keijzer, M, and van Gemert, MJC, *Modeling the Effect of Wavelength on the Pulsed Dye-Laser Treatment of Port Wine Stains.* Applied Optics, 1993. **32**(4): p. 393-398.
20. Welch, AJ, Wissler, EH, and Priebe, LA, *Significance of Blood-Flow in Calculations of Temperature in Laser Irradiated Tissue.* IEEE Transactions on Biomedical Engineering, 1980. **27**(3): p. 164-166.
21. Duck, FA, *Physical Properties of Tissue: A Comprehensive Reference Book.* 1990, London, UK: Academic.
22. Weaver, JA and Stoll, AM, *Mathematical Model of Skin Exposed to Thermal Radiation.* Aerospace Medicine, 1969. **40**(1): p. 24-30.
23. Lepock, JR, Frey, HE, Bayne, H, and Markus, J, *Relationship of Hyperthermia-Induced Hemolysis of Human-Erythrocytes to the Thermal-Denaturation of Membrane-Proteins.* Biochimica Et Biophysica Acta, 1989. **980**(2): p. 191-201.
24. DeBoer, JF, Lucassen, GW, Verkruysse, W, and VanGemert, MJC, *Thermolysis of port-wine-stain blood vessels: Diameter of a damaged blood vessel depends on the laser pulse length.* Lasers in Medical Science, 1996. **11**(3): p. 177-180.
25. Pfefer, TJ, Choi, B, Vargas, G, McNallly, KM, and Welch, AJ, *Pulsed laser-induced thermal damage in whole blood.* Journal of Biomechanical Engineering-Transactions of the ASME, 2000. **122**(2): p. 196-202.
26. Pickering, JW and van Gemert, MJC, *585 Nm for the Laser Treatment of Port Wine Stains - a Possible Mechanism.* Lasers in Surgery and Medicine, 1991. **11**(6): p. 616-618.